Epilepsy & Behavior 22 (2011) S36–S43

Contents lists available at SciVerse ScienceDirect

Epilepsy & Behavior

journal homepage: www.elsevier.com/locate/yebeh

A machine-learning algorithm for detecting seizure termination in scalp EEG

Ali Shoeb [a,*], Alaa Kharbouch [b], Jacqueline Soegaard [c], Steven Schachter [d], John Guttag [b]

[a] Department of Neurology, Massachusetts General Hospital, Boston, MA, USA
[b] Department of Electrical Engineering and Computer Science, Massachusetts Institute of Technology, Boston, MA, USA
[c] Department of Bioengineering, Massachusetts Institute of Technology, Boston, MA, USA
[d] Neurotechnology Program, Center for Integration of Medicine and Innovative Technology, Boston, MA, USA

ARTICLE INFO

Article history:
Revised 27 August 2011
Accepted 29 August 2011

Keywords:
Seizure detection
Machine learning
Seizure termination
Postictal state

ABSTRACT

Efforts to develop algorithms that can robustly detect the cessation of seizure activity within scalp EEGs are now underway. Such algorithms can facilitate novel clinical applications such as the estimation of a seizure's duration; the delivery of therapies designed to mitigate postictal period symptoms; or detection of the presence of status epilepticus. In this article, we present and evaluate a novel, machine learning-based method for detecting the termination of electrographic seizure activity. When tested on 133 seizures from a public database, our method successfully detected the end of 132 seizures within 10.3 ± 5.5 seconds of the time determined by an electroencephalographer to represent the electrographic end of seizure. Furthermore, by pairing our seizure end detector with a previously published seizure onset detector, we could automatically estimate the duration of 85% of test electrographic seizures within a 15-second error margin compared with electroencephalographer determinations.

This article is part of a Supplemental Special Issue entitled The Future of Automated Seizure Detection and Prediction.

1. Introduction

Much effort has been devoted to developing computerized algorithms for detecting the presence of seizure activity within continuous recordings of scalp and intracranial EEGs. Published algorithms include patient-specific [1,2] and nonspecific [3,4] methods capable of detecting seizure events or their onsets in either an online [1,3] or offline [5,6] fashion. Important clinical applications potentially enabled by these algorithms include initiating diagnostic procedures like ictal SPECT [7], delivering neurostimulation [8], and alerting caregivers or family members.

Although some effort has been devoted to developing a method to detect the end of the stereotyped and generalized seizures that are induced by electroconvulsive therapy [9,10], almost no effort has been devoted to creating an algorithm that can reliably detect the end of the electrographic activity associated with epileptic seizures (an electroencephalographic seizure is hereafter referred to as *seizure* unless otherwise specified). This is notable inasmuch as an algorithm with these capabilities might facilitate novel clinical applications. For instance, pairing a seizure onset dector with an end detector could enable the measurement of seizure durations that, when combined with estimates of seizure frequency, could help physicians better assess the efficacy of various types of anticonvulsants or neurostimulation devices. Furthermore, such a detector could notify a family member, caregiver, or emergency services of the potential presence of status epilepticus if a seizure's end is not detected within, for example, 5 minutes of its onset. Finally, being able to detect a seizure's end, which coincides with the onset of the postictal period, could facilitate the development of a device designed to decrease the behavioral and cognitive side effects that accompany the postictal period [11], which can persist anywhere from minutes to days following a seizure [12], or enable a family member to administer such a therapy.

Implicit within some of the literature on automated seizure onset detection using scalp EEGs is the assumption that seizure termination corresponds to the point in time when a detection algorithm lowers its alarm. This assumption may often be false. Seizure onset detectors may lower their alarm when a seizure begins to exhibit ictal activity that is distinct from that of the onset [13].

More generally, using the same decision rule (e.g., a seizure onset decision rule) to signal both the onset and end of a seizure could yield poor results because the characteristics of EEGs that signal the onset of a seizure can be very different from those that signal its end. Seizures with focal activity following their onset may exhibit generalized activity toward their end; conversely, generalized seizures may exhibit focal activity at their end [14]. Furthermore, the rhythmic activity accompanying the onset of a seizure typically has a fundamental frequency within the alpha, beta, theta, or delta band [4], whereas EEGs following seizure termination, which we refer to as postictal EEGs, often exhibit delta wave

* Corresponding author.
E-mail address: ashoeb81@gmail.com (A. Shoeb).

1525-5050/$ – see front matter © 2011 Elsevier Inc. All rights reserved.
doi:10.1016/j.yebeh.2011.08.040

slowing, amplitude attenuation, or a combination of these phenomena [14]. Finally, EEGs following a seizure may immediately revert to the patient's electrographic interictal baseline, which may have morphological abnormalities that are similar to ictal patterns [14].

Detection of both seizure onset and end is further complicated at times by the gradual nature with which the EEG changes at the beginning and end of seizures or by the masking effect of muscle and movement artifacts. When interictal-to-ictal and ictal-to-postictal EEG transitions are gradual or obscured by artifact, electroencephalographers as well as algorithms may be challenged to identify the time of seizure onset and termination.

As an example of the differences between EEGs following seizure onset and offset, consider Figs. 1 and 2. The seizure begins in Fig. 1 just before 2855 seconds with low-amplitude, 10- to 12-Hz rhythmic activity restricted to channels F7–T7, T7–P7, and P7–O1. Seventy seconds later, the seizure terminates at approximately 2925 seconds with high-amplitude, 1- to 2-Hz rhythmic activity that involves all channels as shown in Fig. 2.

Like that for seizure onset [15,16], the EEG immediately following seizure offset varies across patients and seizure types. For example, the EEG in Fig. 3 exhibits generalized amplitude attenuation following seizure termination at approximately 3380 seconds. In contrast, the EEG immediately following the seizure in Fig. 4, which terminates at 1843 seconds, reverts to an abnormal baseline that exhibits periodic runs of 1- to 2-Hz spike-and-wave discharges.

In this article we describe a novel method for detecting the end of seizure activity. Our method, which can be patient specific or nonspecific, involves initiating a search for the end of a seizure once its beginning has been identified; the latter can be accomplished using previously published methods [4,13,15,16]. By separating the tasks of seizure onset detection and seizure end detection, we permit each detector (onset, offset) to be tailored for its assigned task. Furthermore, we reduce the task of seizure end detection to discriminating between ictal and postictal EEG, as opposed to differentiating between interictal, ictal, and postictal EEG.

To identify the end of a seizure, we use a classifier to determine whether feature vectors extracted from an EEG epoch are more similar to ictal or postictal EEG. The feature vector we use is novel in that it summarizes the spectral and spatial characteristics of EEG in a manner that enables the classifier to be robust to changes in the propagation of ictal activity or the spatial distribution of postictal rhythms.

2. Methods: Seizure end detection algorithm

The seizure end detector performs a sliding window analysis of the EEG once a seizure onset detector detects the beginning of a seizure.

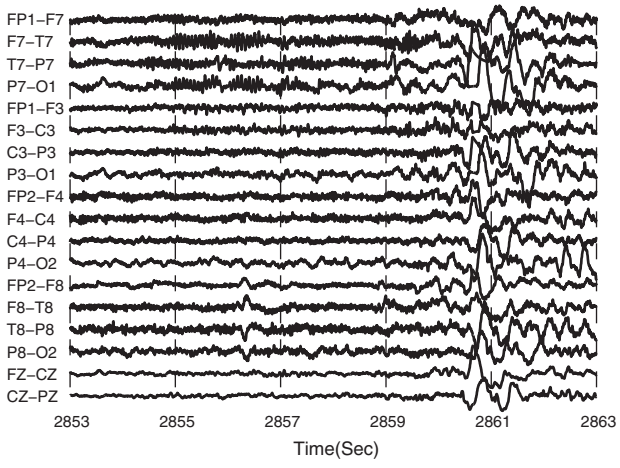

Fig. 1. Example of seizure onset EEG: The seizure begins at 2855 seconds with low-amplitude, 10- to 12-Hz rhythmic activity restricted to channels F_7–T_7, T_7–P_7, and P_7–O_1.

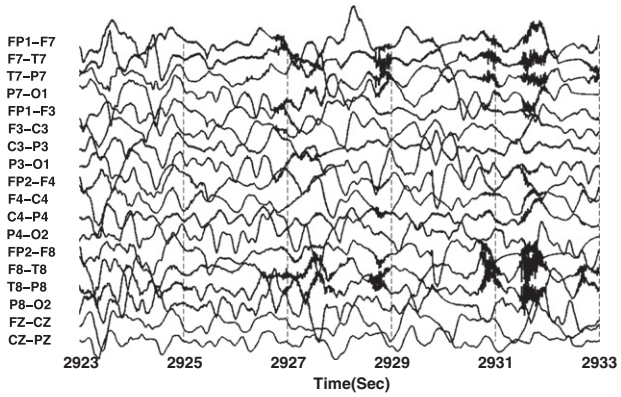

Fig. 2. Example of postictal EEG: The seizure ends at approximately 2925 seconds with high-amplitude, 1- to 2-Hz rhythmic activity that involves all channels.

The analysis window used by the seizure end detector is 5 seconds long and is advanced forward in 1-second increments. The detector extracts salient features from each analysis window, and then assembles those features into a feature vector **X**. Next, the detector uses a classifier to determine whether **X** is representative of the ictal or postictal state. If $L=5$ successive feature vectors are classified as belonging to the postictal state, then the detector declares that the seizure has ended. In the following subsections, we discuss both feature vector extraction and classification.

2.1. Feature vector design

As ictal and postictal EEG activity characteristically differ in both spatial distribution and spectral structure, it is important that our feature vector captures these signal properties. To encode the spectral structure of EEG activity, we measure for each channel $j = 1, 2, \ldots N$ the energy within $M=25$ contiguous frequency bands. The frequency bands are 1-Hz wide and span the frequency range 0–M Hz. The energy in band i on channel j is assigned to the variable x_{ij}.

To compute x_{ij}, we compute the periodogram of channel j, and then sum the values of that function over the indices corresponding to the frequency band i. We estimate the periodogram of an epoch from channel j by applying the Welch algorithm with 1-second window, 50% overlap, and $N_{FFT}=4096$.

A simple and comprehensive way to encode the spatial distribution of EEG activity involves forming an MN-dimensional feature vector by stacking in a column all the spectral energies x_{ij}. This method

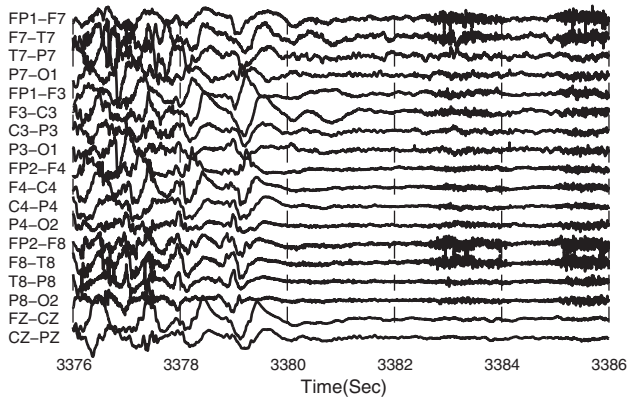

Fig. 3. Example of postictal EEG: The seizure ends at approximately 3380 seconds with generalized amplitude attenuation.

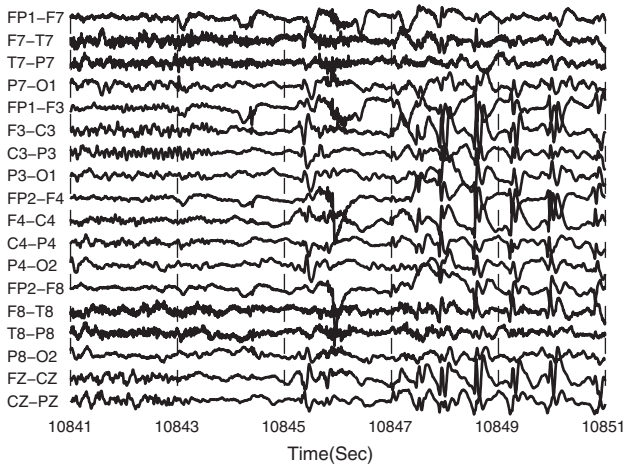

Fig. 4. Example of postictal EEG: Following seizure termination at 1843 seconds, the EEG exhibits abnormal periodic runs of 1- to 2-Hz spike-and-wave discharges, which is consistent with this patient's baseline EEG.

has been shown to work well for detecting seizure onset [16]. It works less well for detecting seizure termination. The problem is sensitivity to changes in the spatial distribution of EEG activity. More specifically, shifts, expansions, or contractions in the spatial distribution of ictal or postictal activity, which result from a change in a seizure's propagation pattern, could translate into large shifts of the feature vector within the feature space. These large shifts can cause a detector to misclassify the extracted feature vector and, as a result, declare seizure termination too early or too late.

To incorporate spatial information without being overly sensitive to spatial shifts in ictal and postictal activity, we construct feature vectors by weighting and averaging features across channels. More specifically, we produce an M-dimensional vector $\mathbf{X}$ whose ith element $\mathbf{X}_i$ is computed by weighting and averaging the energies x_{ij} across N channels as shown below.

$$\mathbf{X}_i = \frac{\sum_{j=1}^{N} w_j x_{ij}}{\sum_{j=1}^{N} w_j}$$

When used in a patient nonspecific context, no a priori information is available to guide the differential weighting x_{ij}, so $w_j = 1$ for $j = 1,2,\ldots,N$. By contrast, in a patient-specific context, channels are weighted based on how differently they appear in the ictal and postictal epochs. If $\bar{x}_{ij,ictal}$ and $\bar{x}_{ij,postictal}$ are the mean x_{ij} extracted from a patient's training ictal and postictal epochs, then the weight for channel j is set to be

$$w_j = \sum_{i=1}^{M} \left| \bar{x}_{ij,ictal} - \bar{x}_{ij,postictal} \right|$$

In summary, we capture the spatial and spectral properties of an EEG epoch using an M-dimensional vector $\mathbf{X}$. The elements of this feature vector correspond to a weighted average, across N EEG channels, of the energy within M contiguous frequency bands.

2.2. Feature vector classification

To classify $\mathbf{X}$ as representative of ictal or postictal activity, we use the Support-Vector Machine (SVM) algorithm [17], specifically, the implementation in the Statistical Pattern Recognition Toolbox (STPRTool) [17]. The SVM algorithm uses training ictal and postictal feature vectors to learn a decision boundary that separates these two classes of activity. In a patient-specific scheme, training ictal and postictal vectors are derived from multiple seizures of a single patient. In the patient nonspecific scheme, training vectors are derived from multiple patients other than the test patient. Once a decision boundary is learned, the SVM algorithm determines the class membership of a newly observed feature vector based on which side of the boundary the vector falls. The SVM algorithm can be used to derive linear or nonlinear decision boundaries. The choice of boundary type depends on both the amount of training data available and the distribution of data within the feature space.

In the patient-specific setting, the amount of training data is limited. Consequently, the use of nonlinear boundaries that tightly fit the distribution of the training samples may result in poor performance on seizures not well represented by the training data. As an example, Fig. 5 shows a two-dimensional projection of training ictal and postictal vectors from a single patient. Fig. 5 also shows the linear and nonlinear decision boundaries learned by the SVM algorithm. If the nonlinear boundary is used, then a test vector that falls within the region it encloses will be classified as representative of ictal EEG; otherwise, the vector will be classified as postictal EEG. If the linear boundary is used, then a test vector that falls below the boundary is classified as ictal EEG.

When compared with the linear boundary, it seems that the nonlinear boundary will correctly classify more test vectors because it correctly separates a greater number of the training vectors. This will indeed be the case provided that the spatial and spectral structure of test seizures remains similar to that of the seizures used to generate training vectors. Now consider how both boundaries perform when used to classify test vectors extracted from the EEG of the same patient, but while the patient was experiencing a seizure type, for example, secondarily generalized seizures, that occurs less commonly than the patient's usual seizure type, for example, complex partial seizures. The test seizure begins like those in the training set, but then evolves so that many of the vectors exhibit spectral and spatial characteristics that differ from those of the training seizures.

Fig. 6 shows how the feature vectors extracted from the test seizure are distributed relative to the training vectors and learned decision boundaries. In this case, the nonlinear boundary correctly classifies the first 15 seconds of the seizure, and misclassifies the remaining stages of the seizure. As a result, the nonlinear boundary incorrectly concludes that the test seizure ends after 15 seconds. In contrast, the linear boundary correctly classifies all but one of the test vectors, and would detect seizure offset with far greater accuracy. So, while the nonlinear boundary exhibits better performance on seizures similar to those of the training set, the linear boundary is more

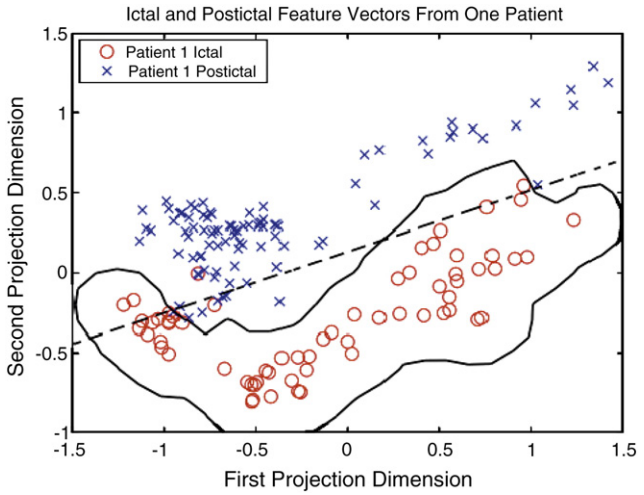

Fig. 5. Linear and nonlinear decision boundaries separating ictal and postictal feature vectors from a single patient.

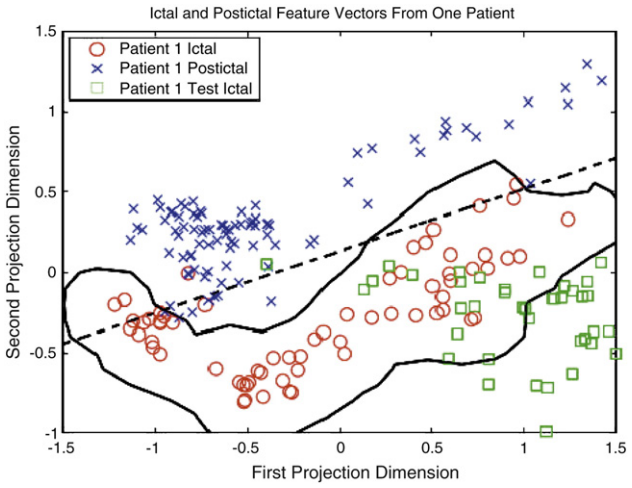

Fig. 6. With limited training data, a linear decision may classify test ictal feature vectors with greater accuracy than a nonlinear decision boundary.

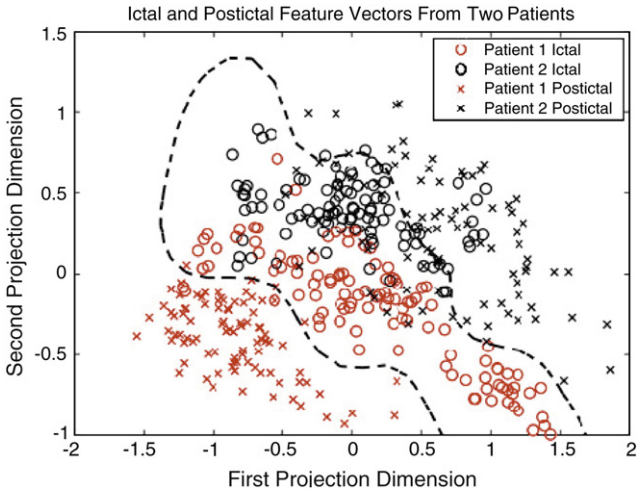

Fig. 8. Nonlinear boundary separating ictal and postictal feature vectors from two patients.

likely to correctly classify seizures that only slightly resemble the training seizures because it does not attempt to tightly circumscribe the training vectors. Because the number of training seizures available for each patient in our database is small, we choose to use a linear decision boundary in the patient-specific setting. More specifically, we use a L_2 soft-margin SVM (*svm2* in STPRTool) with a linear kernel and regularization constants $C=5$ for ictal and $C=1$ for postictal when operating the detector in the patient-specific mode.

In the patient nonspecific setting, training data sets exhibit greater within-class diversity and between-class overlap. Consequently, ictal and postictal feature vectors cannot be well separated by a linear boundary. As an example, Fig. 7 shows a two-dimensional projection of training ictal and postictal feature vectors from two patients. Considering the data of each patient independently, the ictal and postictal feature vectors can be well separated by a linear decision boundary. In other words, the ictal data of patient 1 (red circles) can be linearly separated from the corresponding postictal data (red crosses), and the ictal data from patient 2 (black circles) can also be linearly separated from the corresponding postictal data (black crosses). However, ictal and postictal feature vectors cannot be linearly separated when data from both patients are combined; that is, red and black circles cannot be separated from red and black crosses by a linear boundary. However, as shown in Fig. 8, a nonlinear boundary can separate ictal feature vectors (circles) from postictal vectors (crosses) reasonably well. In this work, we use a L_2 soft-margin SVM with radial basis function kernel, kernel parameter 0.25, and default regularization constants when operating the detector in the patient nonspecific mode.

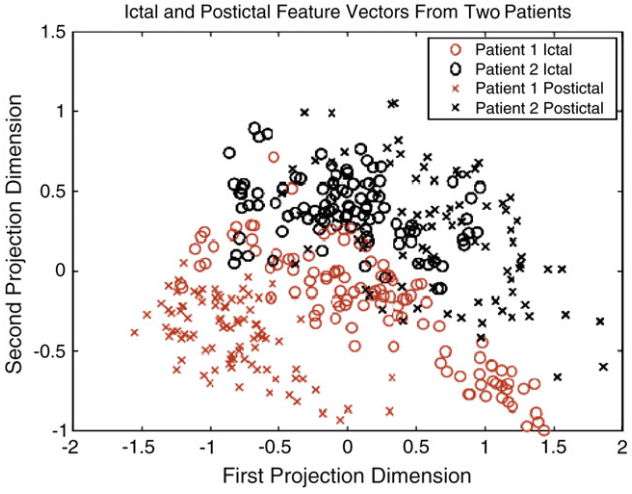

Fig. 7. Ictal and postictal feature vectors from two patients.

3. Testing methodology

3.1. Data set

We evaluated our methodology on the CHB-MIT database (http://physionet.org/physiobank/database/chbmit/). This database contains 133 seizures recorded from 22 pediatric epilepsy patients admitted to Children's Hospital Boston. During their hospital admission, 7 of the patients had partial-onset seizures recorded, 7 had secondarily generalized seizures, and 8 had generalized seizures. The seizures were digitally recorded using a 10–20 bipolar montage and a sampling rate of 256 Hz. For each seizure in the database, a board-certified electroencephalographer determined seizure onset and end times by examining the EEG without knowledge of the determinations made by the algorithm. Fig. 9 shows the minimum, maximum, and mean seizure lengths (duration) for each patient. The numeral over each column indicates the number of seizures available for each patient.

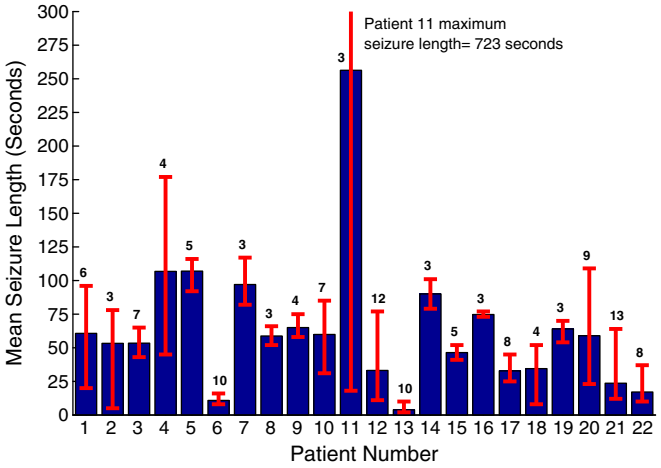

Fig. 9. Minimum, maximum, and mean seizure lengths for each database patient. Each column represents the mean length of a patient's seizures. The lower and upper ends of each vertical line represent the minimum and maximum lengths of a patient's seizures. The numeral over each column corresponds to the number of seizures available for each patient.

3.2. Evaluation metrics

We use multiple metrics to assess the performance of the seizure end detector. The first metric, *offset detection error*, measures the time difference between algorithm declaration of seizure end and expert (electroencephalographer)-marked seizure termination within the EEG. The algorithm declares seizure end at the *end of the last* of $L = 5$ analysis windows that have been successively classified as representative of postictal activity. When we wish to ignore the sign of the error, we report the *absolute end detection error*, which is the absolute value of the end detection error. The second metric, *sensitivity*, refers to the percentage of test seizures whose end the algorithm detected. The third metric, *classification accuracy*, refers to the percentage of ictal and postictal vectors that the end detector correctly classifies. The final metric, *seizure length estimation error*, reflects how well the combination of a patient-specific seizure onset and end detector measures the duration of a seizure. Seizure length corresponds to the interval between algorithm declaration of seizure onset and the *start of the first* of $L = 5$ analysis windows that have been classified as postictal. It is important to note that an accurate estimate of seizure length does not necessarily imply small seizure onset and end detection errors, as onset and end detection errors may be offsetting.

3.3. Evaluation scheme

We use a leave-one-record-out testing procedure to evaluate the performance of our seizure end detector. Because we assume a separate module will detect seizure onset, test records extend from the electrographic onset of a seizure to 90 seconds following its end. Records contain, on average, 64 ± 51 ictal vectors and 90 postictal vectors. Let N_i be the number of records that belong to a patient i.

In the patient-specific context, a seizure end detector is trained on feature vectors derived from the ictal and postictal periods in $N_i - 1$ records. Next, the detector is tasked with detecting seizure end in the withheld record. These two steps are repeated N_i times so that each record from patient i is tested once.

In the patient nonspecific context, a seizure end detector is trained on feature vectors extracted from the records of all database patients other than patient i. Next, the detector is tasked with detecting seizure offsets within all N_i records belonging to patient i.

For each tested record, we note whether seizure offset was detected, and if so, with what error. We also record the percentages of ictal and postictal feature vectors that were correctly classified. Finally, we combine the measured seizure end detection latency with the latency of detecting seizure onset (using an algorithm whose performance on this database has already been published [16]) to determine the error in estimating the duration of the tested seizure.

4. Results

4.1. Seizure end detection error, sensitivity, and classification accuracy

The patient-specific and nonspecific detectors had similar overall performance. The patient-specific detector recognized 132 of 133 seizure ends with a classification accuracy of 90% and an average, absolute end detection error of 10.3 ± 5.5 seconds. The patient nonspecific detector recognized all seizure ends with a classification accuracy of 84% and an average, absolute error of 8.9 ± 2.3 seconds.

Fig. 10 shows the mean, absolute offset detection error for each detection scheme/patient pair. For 16 of 22 patients (e.g., patients 1–3, 5, 7–10, and 13–20) the patient-specific and nonspecific detectors exhibited absolute errors that differed by less than 5 seconds. For the remaining 6 subjects (patients 4, 6, 11, 12, 21, and 22), the absolute detection errors of the two detectors differed by more than 5 seconds. For 4 of these 6 cases, the patient nonspecific detector had the smaller of the two detection errors.

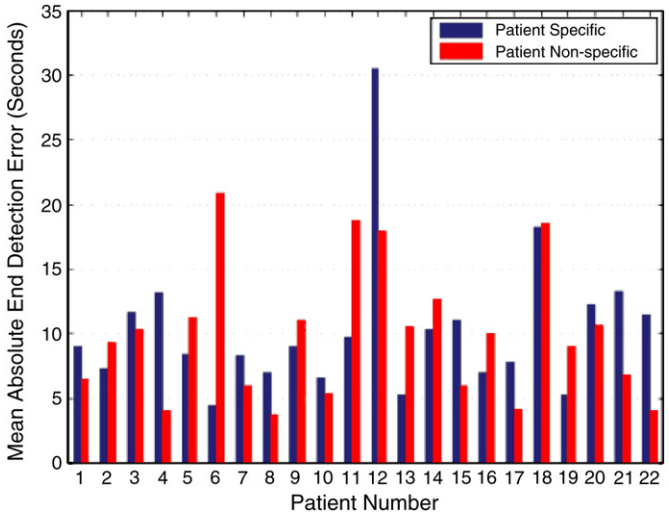

Fig. 10. Patient-specific and nonspecific mean, absolute end detection errors.

Fig. 11 shows histograms of the signed end detection error for the patient-specific and nonspecific detectors. The histograms were constructed using the end detection error recorded for each of the 133 test seizures. For both detectors the majority of seizure ends were detected after the end marked by the expert, which results in a positive error. Each detector noted the end of 81% of the test seizures within 15 seconds of the offset marked by the expert.

Fig. 12 illustrates the classification accuracy for each detection scheme and each patient. The patient-specific detector exhibited accuracy greater than 85% for 18 of 22 subjects, whereas the patient nonspecific detector exhibited the same accuracy for 15 of 22 subjects. The patient-specific detector recorded a greater accuracy than the patent nonspecific detector for 17 of 22 subjects.

4.2. Seizure length estimation

Fig. 13 illustrates a histogram of the signed seizure length estimation error obtained using the combination of an already published patient-specific seizure onset detector [16] and the end detector described in this article. The histogram was constructed using the seizure length estimation error recorded for each of the 133 test seizures. The combined patient-specific seizure onset and end detector estimated the length of 85% of the test seizures within a 15-second

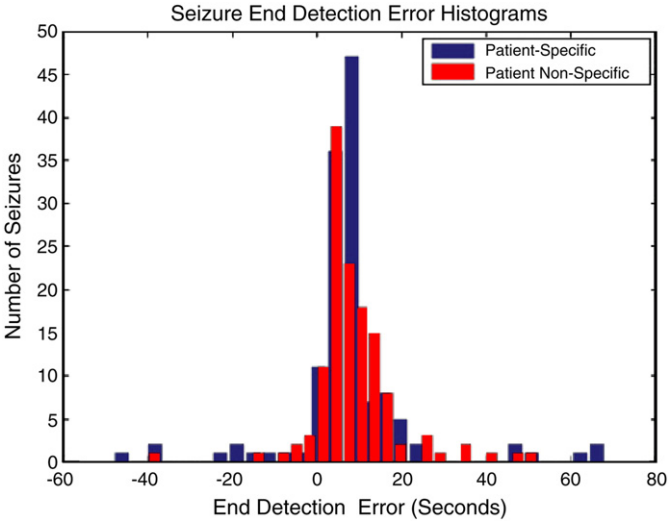

Fig. 11. Histogram of patient-specific and nonspecific end detection errors.

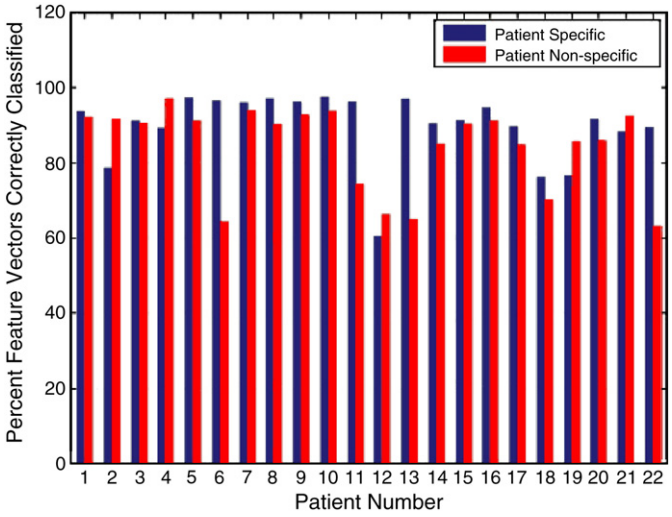

Fig. 12. Patient-specific and nonspecific seizure classification accuracy.

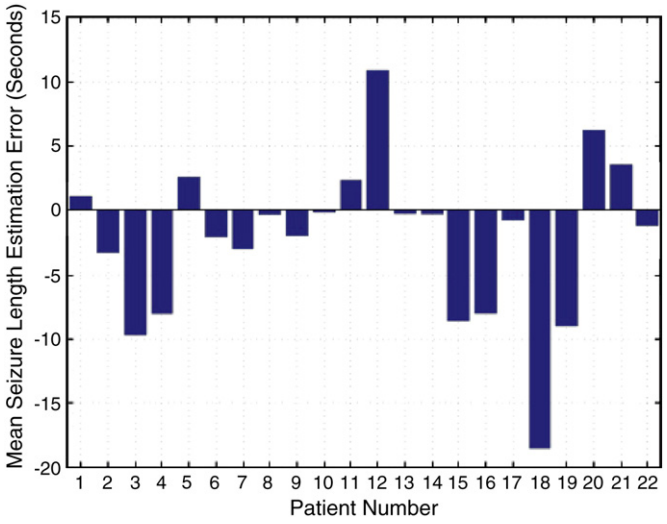

Fig. 14. Mean seizure length estimation error obtained using a patient-specific seizure onset and end detector.

error margin, 93% of the test seizures within a 30-second error margin, and 100% of the test seizures within a 62-second error margin. Although further work will likely reduce this error margin, it would nonetheless be useful clinically as envisioned in the Introduction, especially to signal the potential presence of status epilepticus.

Fig. 14 shows the mean signed seizure length estimation error for each of the 22 test patients. The combined onset and end detector was able to accurately estimate the length of both short seizures (patients 6 and 13) and long seizures (patients 5 and 7). The patients for whom the mean seizure length estimation error was close to or greater than 10 seconds (patients 3, 12, and 18) did not have unusually long seizures or a small number of seizures. Instead, the EEGs of these patients exhibited ictal or postictal activity that caused the end detector to declare seizure termination too early or too late as illustrated in the following section.

5. Case study

The excellent performance of the patient-specific seizure end detector on patient 11 illustrates the detector's robustness to changes in the morphology, location, and duration of a patient's ictal activity. The database contains three seizures for patient 11 of lengths 18, 28, and 723 seconds. As shown in Fig. 15, both short seizures exhibited low-amplitude, 4- to 5-Hz activity that is localized to channels FP_1–F_7, F_7–T_7, T_7–P_7, and P_7–O_1, which are located on the left side of the head.

A portion of the long seizure, which posed a health risk and required pharmacological intervention, is shown in Fig. 16. This seizure exhibited high-amplitude, 2- to 3-Hz activity on the channels involved in the shorter seizures and, in addition, the channels (P_4–O_2, T_8–P_8) that are located on the side of the head opposite the short seizures. Although the long seizure involved different spectral content and channels, the detector was able to correctly identify the end of the 723-second seizure with an 11-second end detection error when trained only on the two shorter seizures. We attribute the detector's robustness to the form of the feature vector and decision boundary. The feature vector incorporates spatial information without being too sensitive to spatial shifts in ictal activity by weighting and averaging features across channels. The linear decision boundary correctly classifies seizure activity that only slightly resembles the training seizures because it does not tightly circumscribe the training vectors. Further work could yield an additional detector to determine when a seizure spreads from the initial ictal zone to another, for example, to the contralateral hemisphere.

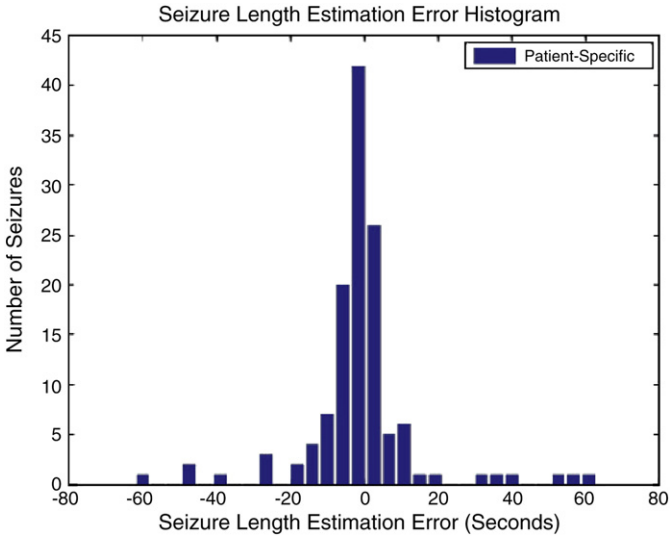

Fig. 13. Histogram of seizure length estimation error obtained using a patient-specific seizure onset and end detector.

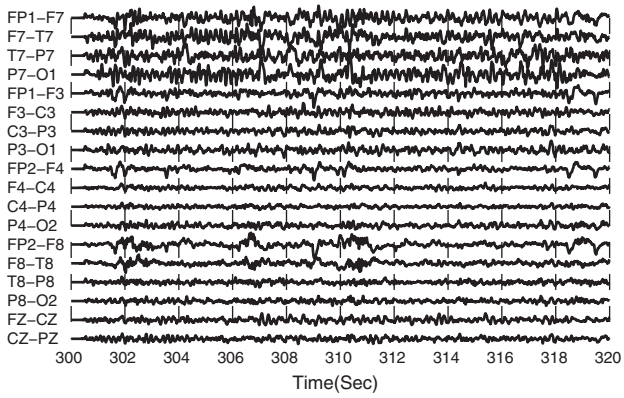

Fig. 15. Seizure activity observed during short seizure of patient 11. Seizures involve low-amplitude, 4- to 5-Hz activity that is localized to the channels FP_1–F_7, F_7–T_7, T_7–P_7, and P_7–O_1.

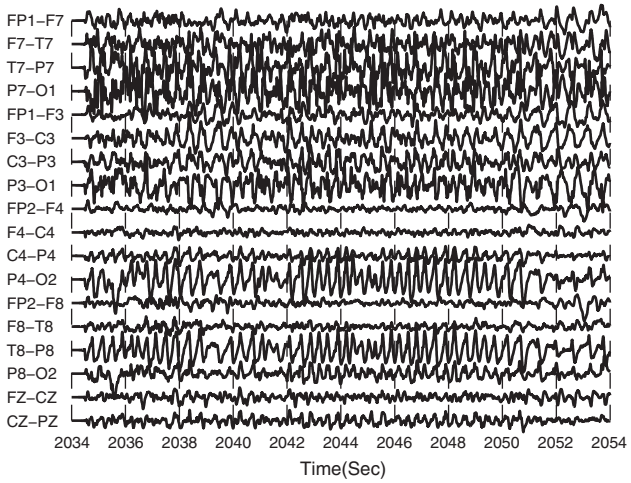

Fig. 16. Seizure activity observed during long seizures of patient 11. The seizure involves 2- to 3-Hz activity on the channels involved in the shorter seizures, and the channels P_4–O_2 and T_8–P_8.

The detector was late in declaring seizure termination whenever a seizure transitioned gradually from the ictal to the postictal state. As an example, Fig. 17 shows a seizure belonging to patient 1. An expert determined that this seizure ends at 1491 seconds because of the simultaneous disappearance of the high-amplitude waves on the channels F_4–C_4, F_8–T_8, and P_8–O_2. However, the character of the rhythmic activity on many other EEG channels (e.g., FP_1–F_7, F_3–C_3, C_3–P_3) changes only slightly following that time point. This caused the algorithm to postpone declaring seizure termination until 1510 seconds, which amounts to a delay of 19 seconds.

In contrast, the detector declared seizure termination prematurely whenever recording or muscle artifacts overlapped seizure activity on multiple EEG channels for longer than $L = 5$ seconds. As an example, Fig. 18 shows a 20-second stretch of artifact-corrupted EEG. The rhythmic ictal activity appears most prominently on channel F_7–T_7 between 1746 and 1750 seconds. In this case, averaging across channels obscures the low-amplitude and spatially localized ictal activity, and causes the detector to incorrectly conclude that the seizure ends 40 seconds before the actual endpoint. This error can potentially be avoided by actively removing artifact-corrupted channels; teaching the seizure offset detector to ignore common artifacts that corrupt ictal EEG; or increasing the period of time (L) the algorithm waits before declaring the end of a seizure.

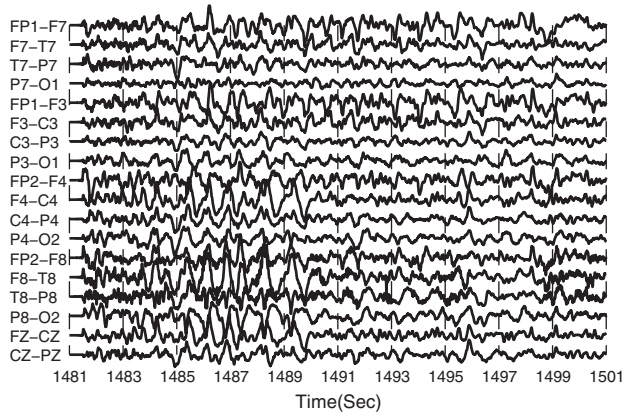

Fig. 17. Similarity in the spectral character of ictal and postictal activity causes the patient-specific seizure end detector to delay declaring seizure termination.

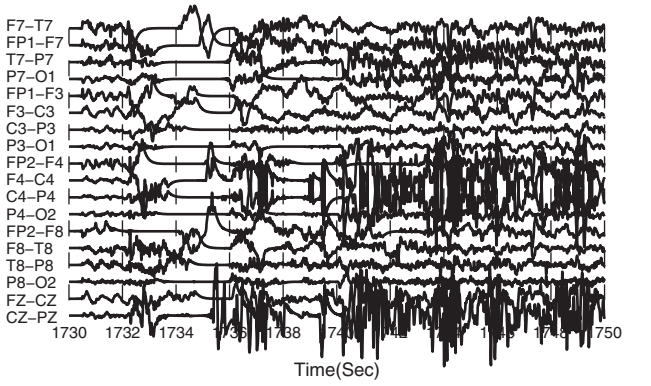

Fig. 18. Recording artifacts cause the seizure end detector to declare seizure termination prematurely.

6. Discussion

To our knowledge, this is the first description and rigorous evaluation of a computerized algorithm for detecting the cessation of epileptic seizure activity using scalp EEG. Our approach separates the task of detecting seizure onset and end, which favorably transforms the problem of seizure end detection. More specifically, seizure end detection is converted from a ternary classification problem that involves distinguishing between interictal, ictal, and postictal EEG to a binary problem that involves separating ictal and postictal EEG.

Feature vector design is crucial to effectively solving a binary classification problem. The feature vector we designed is extracted from a single EEG epoch, and records the mean energy, across channels, within 1-Hz bands spanning 0 to 25 Hz. Averaging across EEG channels is an important step because it enables our classifier to be robust to shifts in the spatial distribution of ictal or postictal EEG. However, restricting feature extraction to a single EEG epoch blinds our detector to the evolution of spectral energy that many seizures exhibit. Therefore, we believe that incorporating features that summarize the relationship between several epochs is worth investigating as it may result in improved seizure end detection.

Also important to solving a binary classification problem is the choice of training data. Patient nonspecific detectors do not required labeled training data from the test patient and are well suited only for patients with common ictal and postictal patterns (e.g., patient 7 whose EEG is shown in Fig. 3). In contrast, patient-specific detectors offer the best performance on patients with uncommon EEG patterns (e.g., patient 6 whose EEG is shown in Fig. 4), but require an electroencephalographer to label training data. It may be possible to reduce the effort needed to deploy a patient-specific detector by using the labels generated by a patient nonspecific detector as training data for a patient-specific detector. In future work, we also hope to investigate whether mixing data from an individual with data from a population of patients results in a detector that can perform well regardless of whether the test patient exhibits common or uncommon EEG patterns.

The database used in this study included numerous patients who experienced both short- and long-duration seizures. However, only patient 11 experienced a 12-minute seizure, which was diagnosed as status epilepticus. Although both the patient-specific and nonspecific detectors estimated the length of this seizure within 15 seconds of error, further testing on cases of status epilepticus are necessary to fully characterize how well our methodology handles these potentially life-threatening seizures. Furthermore, because the CHB-MIT database contains only pediatric EEGs, it is necessary to evaluate the ability of our algorithm to detect the cessation of seizure activity in adult EEGs. We expect the algorithm to perform well because (1) the feature vector used by the algorithm (Section 2.1) includes the spectral bands that capture the majority of the energy in adult

EEGs, and (2) the underlying machine-learning algorithm (Section 2.2) will learn from an adult patient's EEG the relevant spectral and spatial EEG structure that distinguishes ictal from postictal activity.

Finally, the methodology described in this article could potentially be extended to enable the measurement of the duration of the electrographic (but not necessarily clinical) postictal period [14]. More specifically, once the seizure end detector signals the end of the ictal period, another detector may be directed to search for the transition out of the postictal period. The second detector's task will again be reduced to solving a binary classification problem, but this time one that involves separating postictal and interictal EEG.

7. Conclusion

In this article, we described a novel machine learning-based method for detecting the end of seizures. On the tested scalp EEG database, our method exhibits high sensitivity, specificity, and robustness in both the patient-specific and nonspecific settings owing to careful feature vector and classifier design. Furthermore, our detector can easily be paired with previously published seizure onset detectors to facilitate applications such as seizure duration estimation.

Conflict of interest statement

Dr. Shoeb, Dr. Schachter, and Dr. Guttag have licensed a seizure onset detection algorithm to Cyberonics, Inc., and Dr. Schachter and Dr. Guttag are consultants to Cyberonics, Inc.

Acknowledgments

The authors thank the following programs and organizations for supporting this research: the MGH-MIT Career Development Postdoctoral Fellowship in Translational Research; Quanta Computer, Inc.; and the Center for Integration of Medicine and Innovative Technology under U.S. Army Medical Research Acquisition Activity Cooperative Agreements DAMD17-02-2-0006, W81XWH-07-2-0011, and W81XWH-09-2-0001. The information contained herein does not necessarily reflect the position or policy of the government, and no official endorsement should be inferred.

References

[1] Minasyan GR, Chatten JB, Chatten MJ, Harner RN. Patient-specific early seizure detection from scalp electroencephalogram. J Clin Neurophysiol 2010;27:163–78.
[2] Zhang Y, Xu G, Wang J. An automatic patient-specific seizure onset detection method in intracranial EEG based on incremental nonlinear dimensionality reduction. Comput Biol Med 2010;40:889–99.
[3] Aarabi A, Fazel-Rezai R. A fuzzy rule-based system for epileptic seizure detection in intracranial EEG. Clin Neurophysiol 2009;120:1648–57.
[4] Meier R, Dittrich H, Schulze-Bonhage A, Aertsen A. Detecting epileptic seizures in long-term human EEG: a new approach to automatic online and real-time detection and classification of polymorphic seizure patterns. J Clin Neurophysiol 2008;25:119–31.
[5] Chua EC, Patel K, Fitzsimons M, Bleakley CJ. Improved patient specific seizure detection during pre-surgical evaluation. Clin Neurophysiol 2011;122:672–9.
[6] Kelly KM, Shiau DS, Kern RT, et al. Assessment of a scalp EEG-based automated seizure detection system. Clin Neurophysiol 2010;121:1832–43.
[7] Stacey WC, Litt B. Technology Insight: neuroengineering and epilepsy-designing devices for seizure control. Nat Clin Pract Neurol 2008;4:190–201.
[8] Gangadhar B, Dutt D. Automation of seizure duration estimation during ECT; use of fractal dimension. IEEE Eng Med Biol Soc Conf 1995:3.37–8.
[9] Nobler MS, Sackeim HA, Solomou M, et al. EEG manifestations during ECT: effects of electrode placement and stimulus intensity. Biol Psychiatry 1993;34:321–30.
[10] Vonck K, Raedt R, Boon P. Vagus nerve stimulation and the postictal state. Epilepsy Behav 2010;19:182–5.
[11] Fisher RS, Engel Jr JJ. Definition of the postictal state: when does it start and end? Epilepsy Behav 2010;19:100–4.
[12] Polychronaki GE, Ktonas PY, Gatzonis S, et al. Comparison of fractal dimension estimation algorithms for epileptic seizure onset detection. J Neural Eng 2010;7:046007.
[13] So NK, Blume WT. The postictal EEG. Epilepsy Behav 2010;19:121–6.
[14] Hao Qu, Gotman J. A patient-specific algorithm for the detection of seizure onset in long-term EEG monitoring: possible use as a warning device. IEEE Trans Biomed Eng 1997;44:115–22.
[15] Shoeb A, Guttag J. Application of machine learning to epileptic seizure detection. Proceedings, 27th International Conference on Machine Learning (ICML-10); 2010. p. 975–82. [Online]. Available at: http://www.icml2010.org/papers/493.pdf.
[16] Cristianini N, Shawe-Taylor J. An introduction to support vector machines and other kernel-based learning methods. London/New York: Cambridge Univ. Press; 2000.
[17] Franc V, Hlavac V. A new feature of the statistical pattern recognition toolbox. In: Scherer S, editor. Computer vision, computer graphics and photogrammetry: a common viewpoint. Österreichische Computer Gesellschaft; June 2001. p. 143–50. [Online.] Available at: http://cmp.felk.cvut.cz/cmp/software/stprtool/.